Development of an All-Wheel-Drive Tractive System for the 2012 Formula SAE Electric Vehicle

Final Year Thesis Project

David Andrew Ogilvy - 20266654

THE UNIVERSITY OF WESTERN AUSTRALIA

Achieve International Excellence

Table of Contents

Abstract

The UWA Renewable Energy Vehicle Project is developing an electric Formula SAE vehicle inline with a focus on alternative energy sources. This project aims to develop an all-wheel-drive all-electric tractive system for the 2012 FSAE vehicle. The scope of this project covers power systems, feedback control of brushless DC (BLDC) motors, and input signal conditioning.

A number of commercial motor controllers have been investigated for feasibility along with the relevant theory behind controlling BLDC motors. Due to the high power requirements a commercial solution was selected for safety and reliability. Small scale testing was performed with a relatively low power BLDC motor and controller intended for use with remote control aircraft. Various positional feedback encoder designs were investigated for use with the commercial controllers. A common setup using hall effect sensors has been chosen for simplicity but alternatives such as optical encoders have been explored.

Due to the AWD nature of the car with its wheel-hub motors and their independent control, an analogue system has been devised to condition the throttle and brake signals for each controller. This allows for greater stability of the vehicle replacing what would be provided by a mechanical differential gear system. Furthermore, a provision has been made for external modulation of these signals by a drive computer that could utilize a wider range of sensors to provide greater control of each independent motor.

Overall, this project provides the core tractive system while providing a solid basis for future projects.

Acknowledgements

I would like to thank the following people for their support and dedication to the Renewable Energy Vehicle FSAE project:

Professor Dr. Thomas Bräunl for his support and supervision throughout the project.

Brendan Waterman and Stuart Speidel who took on the project as team leaders.

All of the students from the previous years who provided a strong basis for our project through their prior research and development.

All current REV FSAE team members who each contributed greatly to the project through their dedication and many hours spent in the lab working on the vehicle.

The Society of Automotive Engineers, who organize and run the student competition each year, giving us a fantastic opportunity to develop our engineering skills in a fun and competitive environment.

Lastly, I'd like to thank all of our current sponsors who provided us access to their tools, expertise, and products. Such a large project would not have been possible without their support.

Nomenclature

AC – Alternating Current

BLDC – Brushless DC

BEMF – Back Electro-Motive Force

CAN – Control Area Network

DC – Direct Current

ESC – Electronic Speed Controller

FSAE – Formula SAE

PMAC – Permanent Magnet AC

PWM – Pulse Width Modulation

REV – Renewable Energy Vehicle project

SAE –Society of Automotive Engineers

SVM – Space Vector Modulation

List of Figures

List of Tables

Introduction

Beginning in 2011, the University of Western Australia Renewable Energy Vehicle group decided to build an electric FSAE racecar from the ground up. Much of the mechanical design and motor testing had been completed by the end of the year. In 2012, a new team of students took over the project to finalize the designs and actually complete construction of the vehicle. The vehicle has been designed according the explicit rules and regulations set out by the Society of Automotive engineers. This thesis will cover the research and design of the all-wheel-drive tractive drive system for the 2012 competition FSAE vehicle.

Electric Vehicles

With increasing ecological awareness about the pollution from fossil fuel based vehicles, there has been a large push towards developing alternative resource powered transportation. The supply of oil for petrol and diesel is fast becoming a scarce resource with prices continually increasing. In recent years, a number of viable alternatives have been explored including hydrogen power, electric power, and hybrid engines. Out of these, an electric powered vehicle is the most suitable idea for a racecar as it built to race short distances.

Formula SAE Competition

The Society of Automotive Engineers holds a yearly competition for students to compete with each other in student build "Formula SAE" vehicles. The competition is run globally with local chapters of the SAE organizing the events.

2012 UWA REV FSAE Vehicle

The 2012 vehicle was designed from the ground up with a completely new chassis. Rather than having centrally mounted motors that drive the wheels through drive shafts, the decision was made to develop an in-wheel-hub motor and gearing system. Four motors are used, one for each wheel, to create an all-wheel-drive system for superior handling and stability.
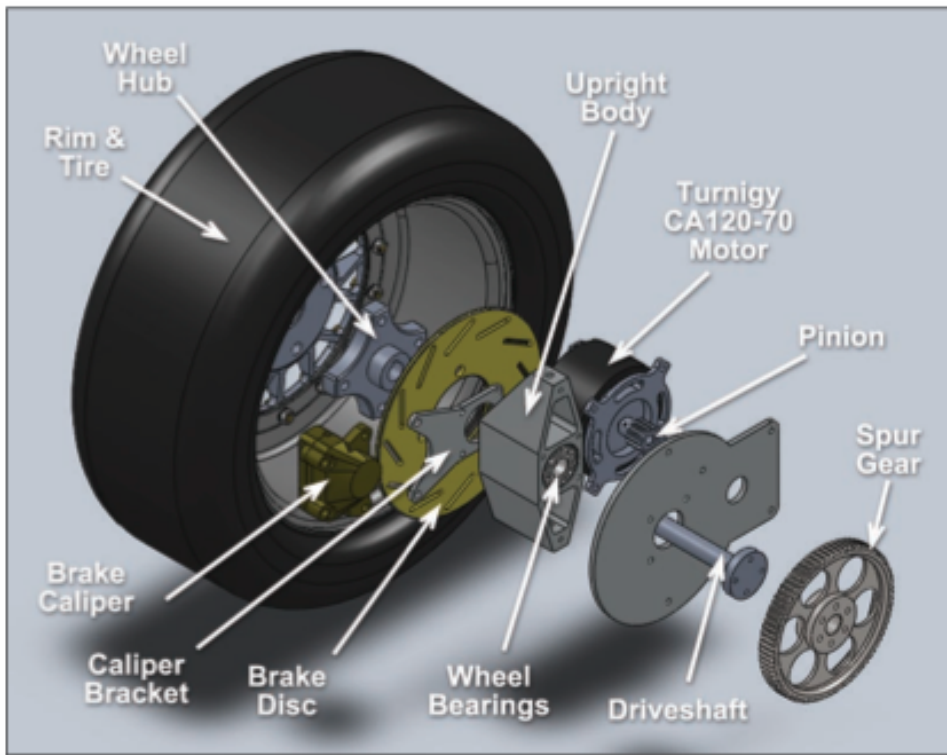
Figure 1. In-wheel-hub motor and gearing design Source [1]

Motor Technology Review

In most cases, electric motors can be subcategorized based on the type of voltage source used to drive them. The two main categories, DC and AC, are briefly reviewed below. A third type, called a brushless DC motor, uses a DC voltage source with electronic control, but the motor construction is firmly based on AC motor theory.

Direct Current (DC) Motors

Direct Current motors are typically powered by a fixed voltage source provided by a battery system or a regulated DC power supply. The motor consists of a fixed stator that provides the constant magnetic field and a rotating rotor that spins the output shaft. The stator is usually made up of one or more pairs of permanent magnets with opposing poles placed on either side of the rotor. The magnetic flux between these poles runs axially through the motor. In some DC motors, the permanent magnets are replaced with field windings to create this magnetic flux region, usually to gain greater flux density or for power control. The rotor is made up of one or more loops of conductive wire. As current I moves through this loop of length L while in the presence of a magnetic field β it experiences a movement force F according to the Lorentz Force Law.

$$F = I \cdot L \times \beta$$
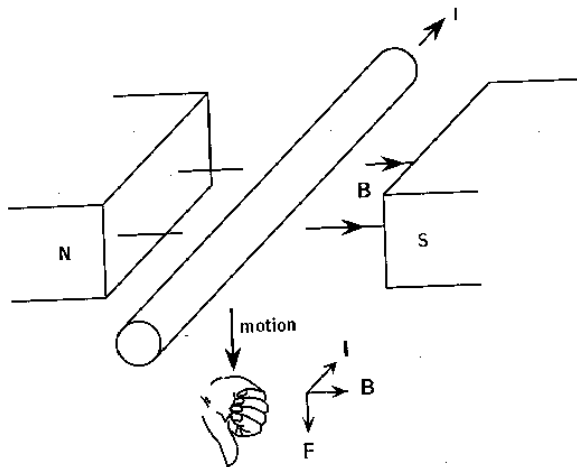
Figure 2. Lorentz Force Law [9]

As the rotor turns, the position of the wire loop changes with respect to the fixed magnetic field, and the induced force turns inwards towards the centre of the rotor, and eventually turns to the opposite direction of the desired rotation due to the

magnetic field being reversed. Reversing the direction of current flow in the coil places the induced force in the correct direction again. Thus, the direction of current must be reversed continuously throughout the rotation. This is achieved through commutation brushes and slip rings. Each brush is connected to the positive and negative side of the DC power source, and the slips rings carry the current to the rotor windings. As the rotor rotates, the slip rings make contact with each brush alternately, effectively reversing the voltage applied through the winding. Most typical DC motors will have multiple magnetic poles and multiple sets of windings to provide smooth power delivery, which necessitates the requirement of multiple sets of slip ring contacts.
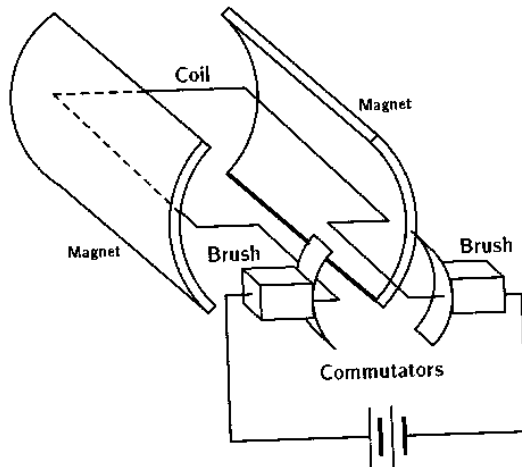
Figure 3. Brushed DC Motor [9]

Alternating Current (AC) Motors

Alternating Current motors are powered from an AC electricity source, which is almost always a sinusoidal waveform. AC motors can be powered by one or more power phases with equally spaced phase delay. Most AC motors are typically single-phase or 3-phase types. As with DC motors, the construction consists or a stator and a rotor. In contrast to DC motors, AC motors typically have fixed stator windings that create a rotating magnetic field. This is possible without commutation as the AC waveform alternates between positive and negative voltage potentials. The fixed magnetic field is created by the rotor utilizing various methods, which is what defines the type of AC motor.

Synchronous Type

Synchronous AC motors are so called because they produce torque at a speed that is synchronous with the line frequency which drives it. Non-excited synchronous motors rely on permanent magnets on the rotor to created the fixed magnetic poles which are driven by the rotating stator magnetic field, or, the rotor can be constructed out of certain types of steel which become magnetized by the rotating magnetic field. At synchronous speeds, the magnetic field through the rotor is constant thus the required magnetic poles are induced. Larger, more powerful AC synchronous motors have a separately DC-excited electromagnet in the rotor. Power to these windings is usually supplied through slip rings similar to those used in DC motors. The synchronous speed n is determined by the line frequency f and the number of pole per phase p as follows:

$$n_{rpm} = \frac{120 \times f}{p}$$

Induction Type

AC induction motors have a winding on the rotor, but no current is applied directly. Instead, current is induced into the rotor by the magnetic field of the stator. If the rotor were to be spinning synchronously with the stator field, then no current would be induced and thus no torque generated. As such, induction motors are asynchronous. The same equation above is used to determine the synchronous speed, and the difference between synchronous speed and the actual rotor speed is called the slip. Typically this value is 1.5-2% for large motors and 4-6% for smaller motors at the full rated load. As the rotor winding has very low resistance, a small slip value induces a large current producing the necessary torque.

$$s = \frac{n_s - n_r}{n_s}$$

AC motors are typically used in fixed speed or fixed load applications as their rotational speed is depending on the supply frequency. The physical construction of the motor is specifically designed to run at the desired rotational speed when running on the 50Hz frequency mains supply.

Brushless DC (BLDC) Motors

Brushless DC motors are unique in that they are not commutated by mechanical means. They are electronically commutated motors that are driven by a DC source through an inverter to produce an AC waveform. The motor design is essentially a permanent magnet synchronous motor with windings on the stator to create the rotating magnetic field. The rotor is made of permanent magnets to create the requisite magnetic poles. BLDC motors can be made up of one or multiple phases although 3-phase is the most common.

Each phase winding has some resistance, some inductance, and when rotating, a BEMF voltage. A mathematical representation of a BLDC motor is shown below.

$$\begin{bmatrix} U_a \\ U_b \\ U_c \end{bmatrix} = \begin{bmatrix} r_a & 0 & 0 \\ 0 & r_b & 0 \\ 0 & 0 & r_c \end{bmatrix} \begin{bmatrix} i_a \\ i_b \\ i_c \end{bmatrix} + \frac{d}{dt} \begin{bmatrix} L_a & M_{ab} & M_{ac} \\ M_{ba} & L_b & M_{bc} \\ M_{ca} & M_{cb} & L_c \end{bmatrix} \begin{bmatrix} i_a \\ i_b \\ i_c \end{bmatrix} + \begin{bmatrix} e_a \\ e_b \\ e_c \end{bmatrix}$$

U_x is the applied voltage across each phase, i_x is the phase current, r_x is the phase resistance, L_x is the phase self inductance, M_{xy} is the phase mutual inductance, and e_x is the BEMF voltage.

BLDC motors are the most promising technology for an electric vehicle as pure electric vehicles, unlike hybrids, source their power directly from DC batteries.

Technology Comparison

Feature	BLDC Motor	Brushed DC Motor
Commutation	Electronic commutation based on Hall position sensors.	Brushed commutation.
Maintenance	Less required due to absence of brushes.	Periodic maintenance is required.
Life	Longer.	Shorter.
Speed/Torque Characteristics	Flat – Enables operation at all speeds with rated load.	Moderately flat – At higher speeds, brush friction increases, thus reducing useful torque.
Efficiency	High – No voltage drop across brushes.	Moderate.
Output Power/ Frame Size	High – Reduced size due to superior thermal characteristics. Because BLDC has the windings on the stator, which is connected to the case, the heat dissipation is better.	Moderate/Low – The heat produced by the armature is dissipated in the air gap, thus increasing the temperature in the air gap and limiting specs on the output power/frame size.
Rotor Inertia	Low, because it has permanent magnets on the rotor. This improves the dynamic response.	Higher rotor inertia which limits the dynamic characteristics.
Speed Range	Higher – No mechanical limitation imposed by brushes/commutator.	Lower – Mechanical limitations by the brushes.
Electric Noise Generation	Low.	Arcs in the brushes will generate noise causing EMI in the equipment nearby.
Cost of Building	Higher – Since it has permanent magnets, building costs are higher.	Low.
Control	Complex and expensive.	Simple and inexpensive.
Control Requirements	A controller is always required to keep the motor running. The same controller can be used for variable speed control.	No controller is required for fixed speed; a controller is required only if variable speed is desired.

Table 1. Comparing a BLDC Motor to a Brushed DC Motor [2]

As can be seen in Table 1, BLDC motors are far superior to brushed DC motors in terms of performance. Brushed DC motors require regular maintenance to inspect and replace the brushes as they wear down from frictional forces due to their mechanical contact. They lose efficiency due to the voltage drop across the brushes and cannot obtain the higher speeds achievable with BLDC motors. BLDC motors can also achieve greater power density for a given frame size, which is vitally important for the FSAE in-wheel-hub design. The only real downside is the higher cost and the complex control requirements.

Features	BLDC Motors	AC Induction Motors
Speed/Torque Characteristics	Flat – Enables operation at all speeds with rated load.	Nonlinear – Lower torque at lower speeds.
Output Power/ Frame Size	High – Since it has permanent magnets on the rotor, smaller size can be achieved for a given output power.	Moderate – Since both stator and rotor have windings, the output power to size is lower than BLDC.
Rotor Inertia	Low – Better dynamic characteristics.	High – Poor dynamic characteristics.
Starting Current	Rated – No special starter circuit required.	Approximately up to seven times of rated – Starter circuit rating should be carefully selected. Normally uses a Star-Delta starter.
Control Requirements	A controller is always required to keep the motor running. The same controller can be used for variable speed control.	No controller is required for fixed speed; a controller is required only if variable speed is desired.
Slip	No slip is experienced between stator and rotor frequencies.	The rotor runs at a lower frequency than stator by slip frequency and slip increases with load on the motor.

Table 2. Comparing a BLDC Motor to an Induction Motor [2]

In comparison with AC induction motors, BLDC motors again have the advantage in power density. Induction motors have a non-linear torque curve with lower torque at low speeds and require large amounts of start up current before they reach a usable speed. The rotor also runs at a lower frequency than the stator and the slip increases with load making it difficult to obtain real speed information. BLDC motors have a much wider usable speed range making them ideal for a vehicle that may be running at full speed all the way down to a slow crawl.

Turnigy CA120-70 BLDC Outrunner Motor

The decision was made in 2011 by the previous REV FSAE team to utilize BLDC motors in the mechanical design and a number of motors were evaluated. Out of these, the Turnigy CA120-70 BLDC Outrunner motor was chosen due to its performance to price ratio. The outrunner design of the motor means the stator is on the inside, with the rotor on the outside. The outer motor can holds the permanent rare earth magnets and is supported by bearings on both ends with a shaft running through the centre. It is a 3-phase BLDC motor with 24 winding slots on the stator. There are 28 magnets evenly spaced around the rotor can making this a 14 pole pair motor. The

16

magnets are arranged facing in alternating directions to achieve alternating north and south magnetic poles.

Figure 4. Turnigy CA120-70 BLDC Motor [11]

Based on limited available specifications from the manufacturer, this motor is capable of 300A peak current with a maximum voltage of 70V. It has an official motor constant kV value of 150 rpm/V which has been previously tested by Ian Hooper to have a real measured value of 147 rpm/V [1]. The kV value of a motor is determined by its design, and represents the no load speed the motor will rotate at with a given voltage.
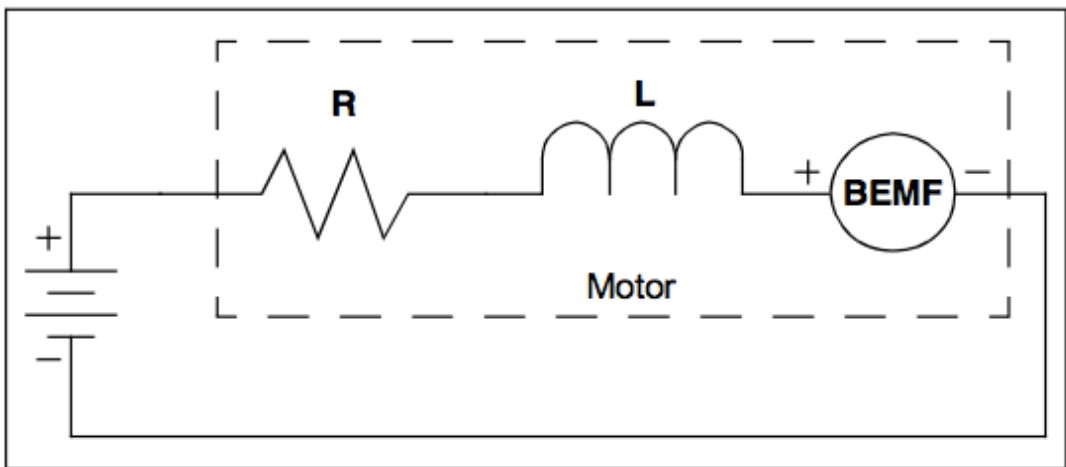
Figure 5. Model Representation of a Single Motor Phase

$$RPM = K_v \times V$$

$$BEMF = \frac{RPM}{K_v}$$

By manually rotating the motor at a fixed speed with an external force, the Kv value can be determined by measuring the BEMF. In this scenario the resistance and inductance of the motor can be ignored as there is no current flow under test.

Figure 6. BEMF Waveform of the Turnigy CA120-70 BLDC Motor

The capture in Figure 6 above shows the BEMF across one phase of the Turnigy motor while it is being rotated by an external force.

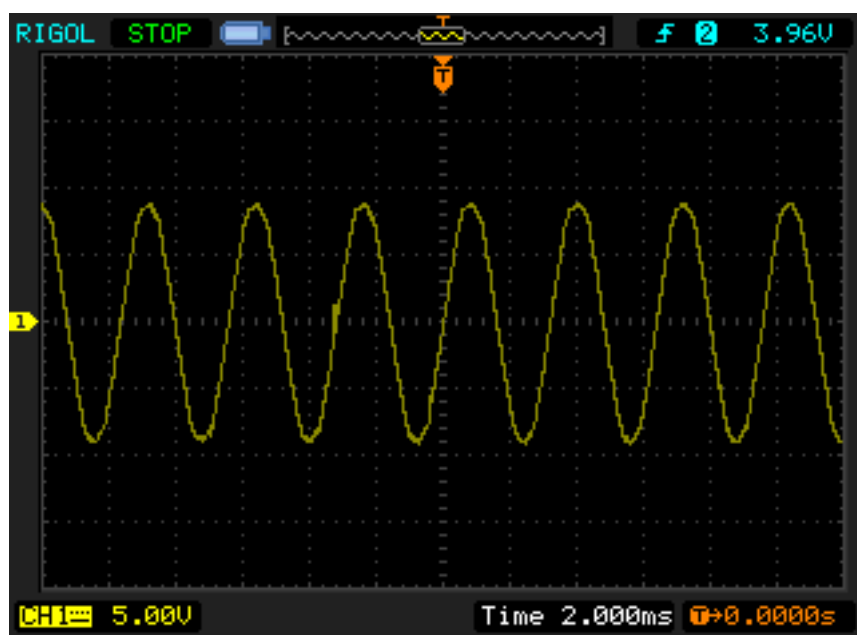The other important characteristic is the motor torque constant Kt. It is measured in units of Nm/Amp and is directly related to the motor constant Kv by the following equation. Note: Kv must be in units of radians/sec/V.

$$K_v \cdot K_t = 1$$

Using a value of Kv = 147 rpm/V (15.386 rad/s/V), calculations reveal a Kt constant of 0.065 Nm/A. Given the peak current rating of 300A, it is expected that the motor can deliver 19.498Nm of peak torque.

The stator winding on the motor is wound according to the distributed LRK design with the following pattern: AabBCcaABbcCAabBCcaABbcC [13]. Note how the pattern repeats twice. The sequence represents the 24 slots in the stator in a clockwise direction. Each letter represents one phase and the capitalization means the wire is wrapped in the opposite direction on that slot. The figure below shows the windings on a 12 slot stator wound in the pattern above. This winding configuration gives the motor a sinusoidal BEMF characteristic as opposed to simpler winding patterns that give a trapezoidal characteristic. It is also important to note that the 3 phases are connected in the delta configuration. The other alternative is the star or wye connection. If the motor were to be connected in a wye configuration, the Kv value would be lower (divided by $\sqrt{3}$) resulting in more torque at low speed, but diminished peak RPM. In delta configuration, the kV value of 147 rpm/V matches up with the FSAE vehicle's maximum battery voltage of 57.6V, giving a theoretical maximum speed of about 8460 RPM. Given that the mechanical design and gearing has already been developed around this specification, there is no advantage to changing to a wye configuration. Top speed would be reduced in order to gain low-end torque.
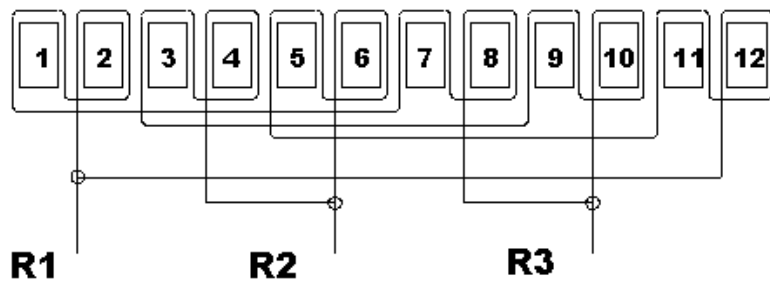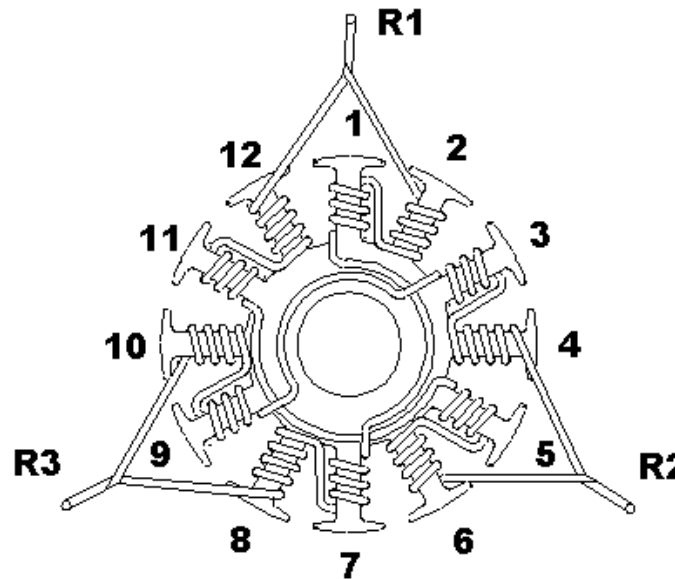
Figure 7. dRLK Winding Pattern – 12 Slot Stator

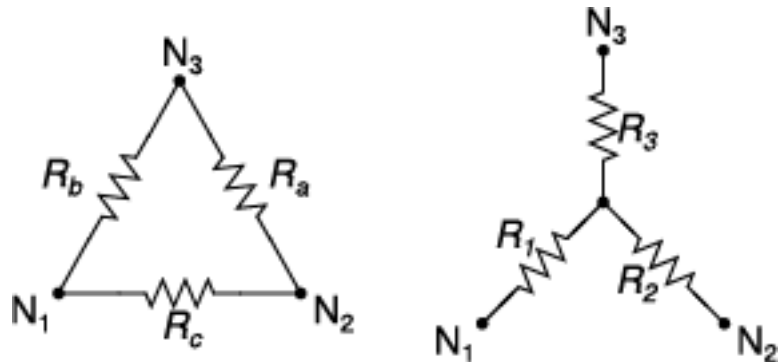*Figure 8. Delta vs Wye connection [10]*

Motor Control Theory

Each different type of motor has its own various control techniques. DC motors can be voltage controlled or PWM controlled. AC motors can be controlled by voltage, rotor field strength, or by a variable frequency controller depending on whether it is power output or speed, which is to be regulated. As the Turnigy BLDC motors have

been chosen for the Formula SAE project, the focus of this section will be on BLDC commutation and control.

Commutation

BLDC motors are not self-commutating by mechanical means like most other motor types. They required electronic control systems to energize each phase in turn. This is achieved through a 3-phase bridge for the most common 3-phase BLDC motor type. The bridge consists of 6 mosfet transistors – one pair per phase. One high side transistor connects the phase connection to the positive DC voltage while one low side transistor connects it to the negative side.
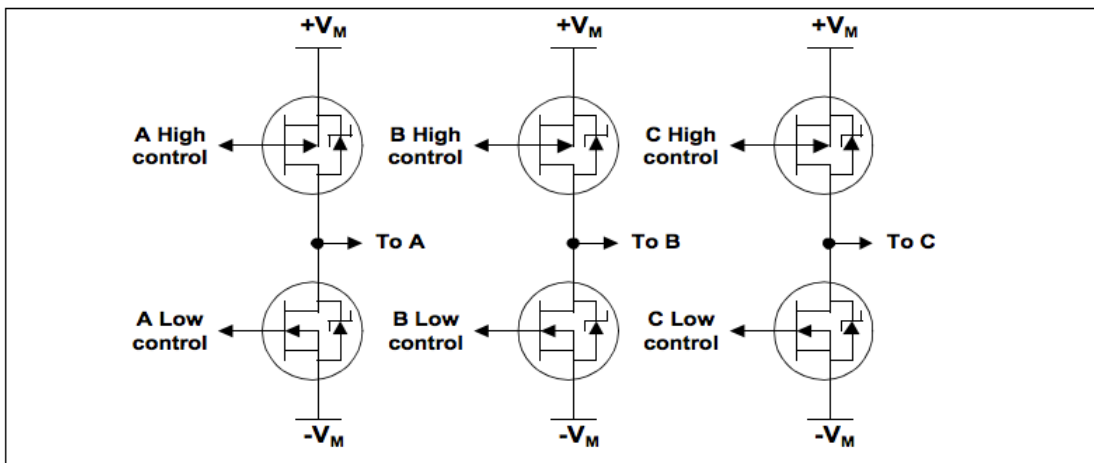

Figure 9. 3-phase 6-MOSFET Bridge [3]

There are six commutation steps per electrical cycle. The first step connects the positive voltage +Vm to motor connection A by turning on the A High control transistor. Motor connection B is then connected to the negative side of the voltage source –Vm by turning on the B Low control transistor. Current now flows in the positive direction through A and out B. The next step allows current to flow from C to B and the third commutation step flows current from C to A. The remaining 3 steps repeat the first 3 steps, but the terminal connections are now reversed. Where terminal A was connected to +Vm in step 1, it is now connected to –Vm in step 4. Likewise, terminal B is connected to +Vm instead of –Vm. Thus, the current flows are now reversed. This is how the rotating magnetic field of the stator is obtained. Note that each phase winding has two slots on the stator that are directly opposite each other. After 180° of electrical rotation, the current reverses and the magnetic flux direction

changes.
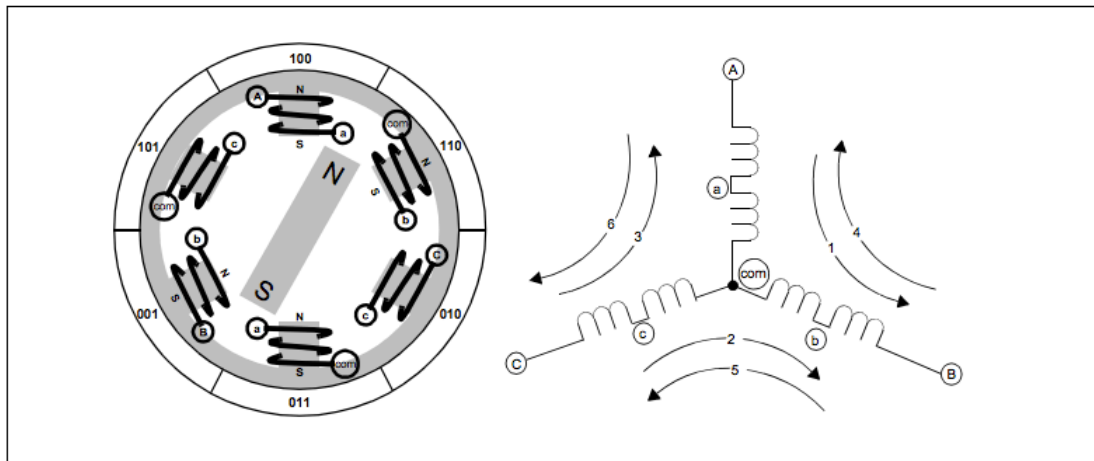
Figure 10. 3-phase BLDC Motor in Wye Configuration [3]

Step	A High	A Low	B High	B Low	C High	C Low	VA	VB	VC
1	ON	OFF	OFF	ON	OFF	OFF	+Vm	-Vm	NC
2	OFF	OFF	OFF	ON	ON	OFF	NC	-Vm	+Vm
3	OFF	ON	OFF	OFF	ON	OFF	-Vm	NC	+Vm
4	OFF	ON	ON	OFF	OFF	OFF	-Vm	+Vm	NC
5	OFF	OFF	ON	OFF	OFF	ON	NC	+Vm	-Vm
6	ON	OFF	OFF	OFF	OFF	ON	+Vm	NC	-Vm

Table 3. Commutation Steps

Figure 11. Phase Voltages throughout Commutation [7]

Figure 12. Flux Vector Rotation during Commutation [7]

In order to effectively commutate the motor, the controller needs to ensure it is applying the correct step depending on the current position of the rotor. It also requires knowledge of the rotational speed so it can transition to the next step with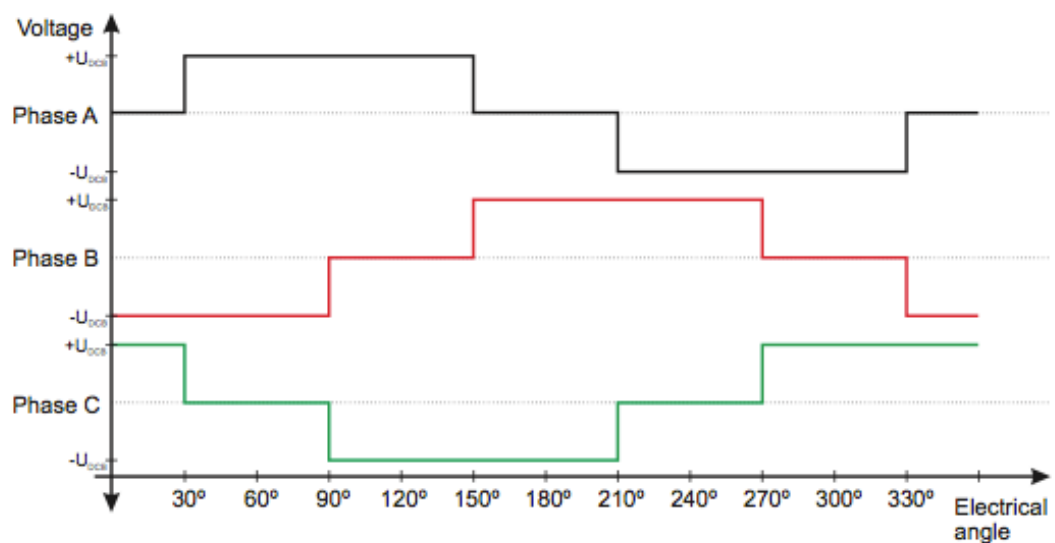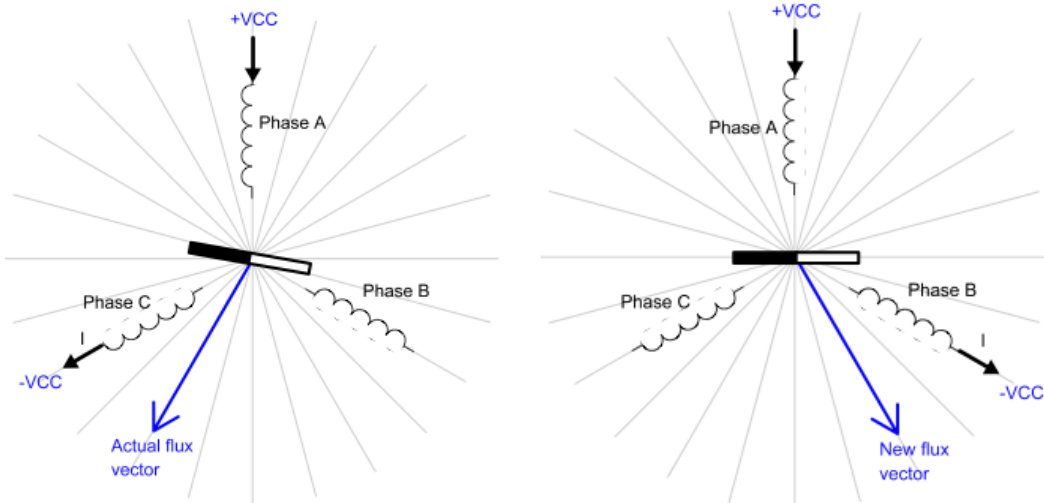 the correct timing. Positional feedback is typically obtained using some form of sensor, but sensor less operation is also possible by monitoring the electrical feedback characteristics of the motor in operation.

Positional Feedback Without Sensors

By measuring the BEMF of the undriven phase, the position of the rotor can be determined. Each of the six commutation steps covers 60° of the electrical cycle. Each of the three phases are only undriven during two of these steps. Half of the DC battery voltage is defined as the virtual ground or the midway point of the sinusoidal BEMF waveform. During each of the two undriven commutation steps, the BEMF waveform makes a zero crossing through this virtual ground point exactly in the middle of the commutation step. By measuring the BEMF of the undriven phase during commutation and detecting the zero crossing point, the controller can determine when to transition to the next commutation step. The next commutation transition occurs 30° after the zero crossing detection.

The controller needs to know the angular velocity of the rotor to correctly time the step advancement. The velocity can be measured by timing successive zero crossings and constantly updates using a wide variety of algorithms. This method of positional

feedback does present a few issues. If the motor changes velocity after the zero crossing then the commutation step transition timing will be incorrect, occurring either too early or too late. During motor start up, the position of the rotor is unknown, and there is no BEMF to measure. At very low start up speeds, the BEMF amplitude is very small making it difficult to detect zero crossings. A typical start up strategy is to simply start commutation from an arbitrary commutation step with a ramp up in commutation speed. This can lead to what is commonly called cogging, when the rotor jerks back and forth until its rotation synchronizes with the commutation speed. Excessive current flows through the windings during the unsynchronized phase.

BEMF sensing control systems are best suited for applications where there is a fixed or relatively small load on the motor during start up. Due to the low BEMF amplitude at low speeds they are not recommended for applications that require use of the full speed range of the motor. As such, this type of control system is not suitable for the Formula SAE vehicle. The vehicle needs to operate throughout the speed range and a large variable demand is placed on the motor at all times.

Positional Feedback With Sensors

The two main types of sensors used for positional feedback are quadrature encoders and hall effect sensors.

Quadrature Encoders

Quadrature encoders are mounted on the output shaft of the motor and provide three output signals. Two phase outputs, A and B, represent the position of the rotor. The third output is an index pulse that occurs once per revolution. Quadrature encoders provide precise positional information but they do not provide the absolute position of the rotor. During start up, the phases of the motor are energized in turn to move the rotor to a known location.
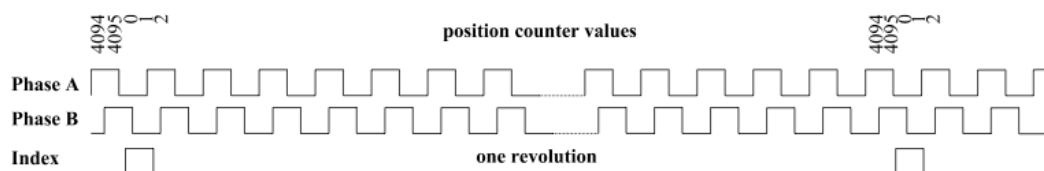

Figure 13. Quadrature Encoder [6]

The full resolution of the encoder is divided up into six sectors corresponding to the commutation steps. The zero position indicated by the index pulse is placed in the correct location by reading the encoder value during the start up sequence.
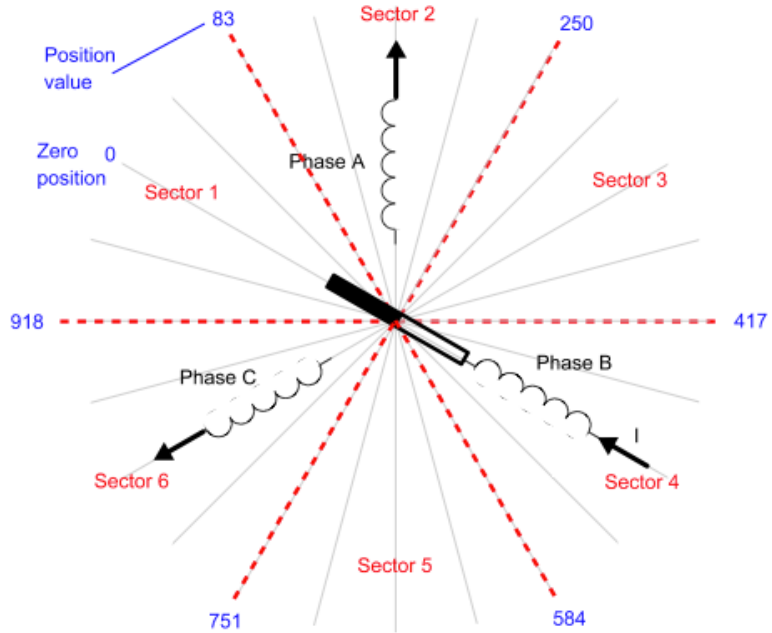
Figure 14. Quadrature Encoder Commutation Sectors [6]

Hall Effect Sensors

Hall effect sensors are semiconductor devices that detect the presence of a magnetic field. A hall effect encoder system consists of three sensors which detect the magnetic field of a magnet which passes across the sensors. The three sensors are equally spaced to cover one electrical rotation. In other motor types, which do not use permanent magnets in the rotor, the sensor is placed on the output shaft. The shaft then has a number of magnets on it matching the pole-pair parameters of the motor. With BLDC motors, it is possible to utilize the existing permanent magnets in the rotor for hall effect sensing.
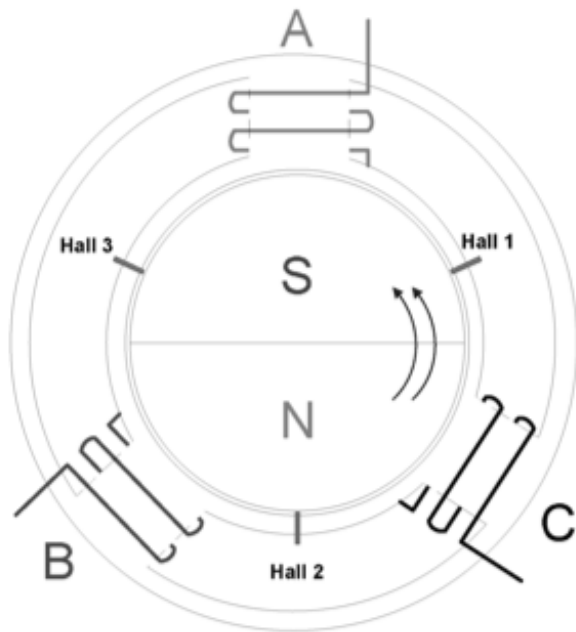
Figure 15. 3-Phase Single Pole Pair Motor – Hall Effect Locations [8]

The hall effect sensors each output a high signal for one magnetic pole, and a low signal for the other magnetic pole. As the rotor advances through one electrical rotation, both the north and south magnetic poles pass across each sensor. The result is a half-duty square wave output with a period corresponding to the electrical frequency. The three sensors are spaced 120° apart. From the figure below, it is quite clear that there are six evenly spaced high/low transitions from the three sensor outputs. Each of these transitions indicates that a commutation step transition should occur.

Figure 16. Hall Effect Signal vs Commutation Timing [3]

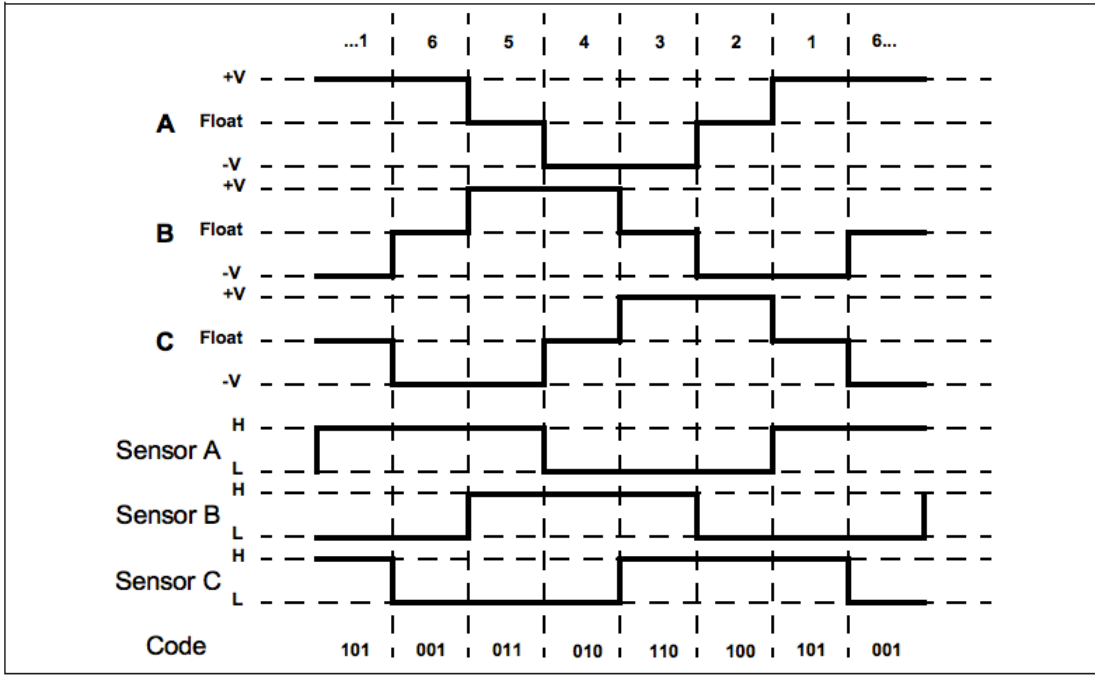The controller has a lookup table which tells it which commutation step should occur during each hall effect encoder state. This table varies by controller, depending on the alignment of the sensors with the rotor and the motor winding connections. A typical configuration is to have hall sensor 1 aligned with the BEMF across the M2-M1 connections, hall sensor 2 aligned with M3-M2, and hall sensor 3 aligned with M1-M3, where M1, M2, and M3 are the output terminals of the controller connected to the phase windings. The hall effect outputs should be a square wave representation of the BEMF. An example table is given below corresponding to the figure above.

Step	Hall A	Hall B	Hall C	Code	A (M1)	B (M2)	C (M3)
1	1	0	1	101	+Vm	-Vm	Float
2	1	0	0	100	Float	-Vm	+Vm
3	1	1	0	110	-Vm	Float	+Vm
4	0	1	0	010	-Vm	+Vm	Float
5	0	1	1	011	Float	+Vm	-Vm
6	0	0	1	001	+Vm	Float	-Vm

Table 4. Commutation vs Hall Input Lookup Table

Speed and Torque Control

Pulse-Width Modulation

With a fixed voltage source, the only way to effectively control the current through the motor windings is to use pulse-width modulation on the gate drive signal for the mosfets in the three-phase bridge. PWM operates by driving the mosfet gate for a short period specified as the turn on time (T_{on}). During the rest of the commutation step the drive signal is low, specified as the turn off time (T_{off}). The ratio of on time to off time is defined as the PWM duty cycle ranging from 0% to 100%. The number of times the PWM drive signal transitions between T_{on} to T_{off} is defined as the PWM frequency. The average current through the motor, and thus the torque, is proportional to the PWM duty cycle.
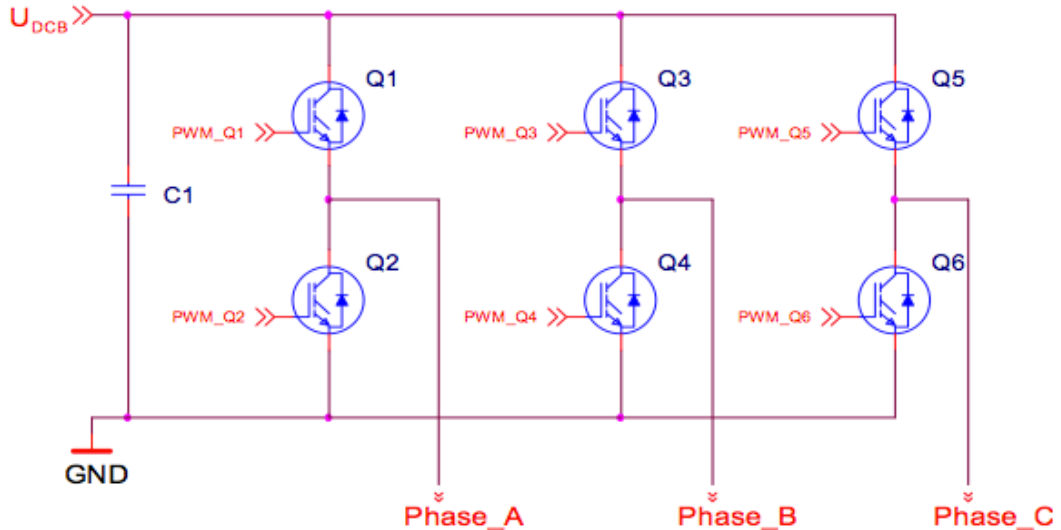

Figure 17. Mosfet Inverter Bridge [6]

Pulse-width modulation can be applied to the high side mosfets, the low side mosfets, or both. An example of PWM being applied to both high and low side mosfets is shown in the figure below.
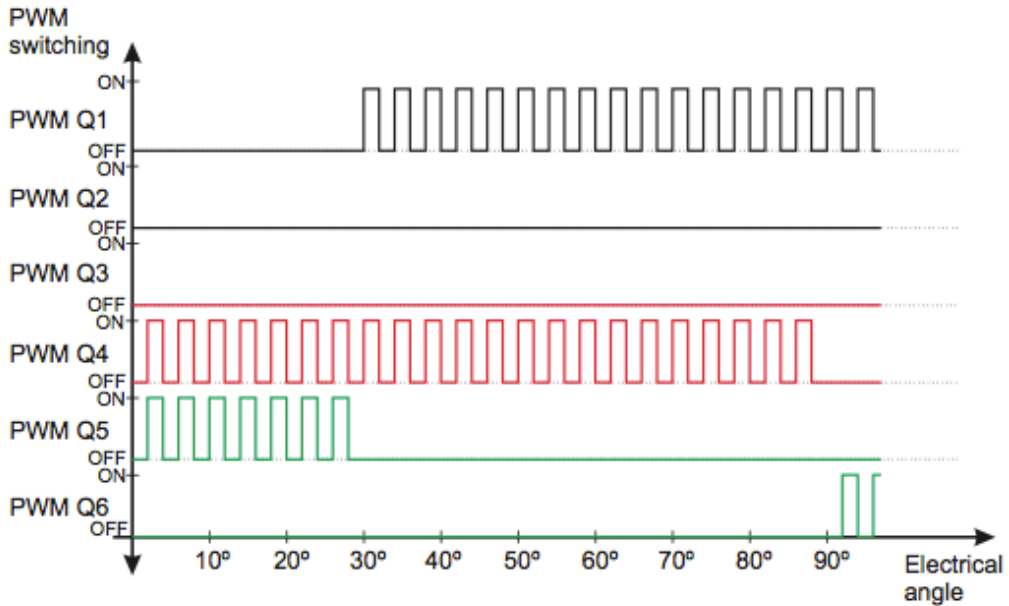
Figure 18. PWM Control Waveforms [6]

Open Loop Control

In open loop control mode, the input speed reference signal is directly translated into a PWM duty cycle value. This is then used by the commutation logic to drive the inverter bridge. The hall effect feedback signal is only used to perform the electronic commutation steps required to drive the motor. There is no real speed reading feedback. The motor stabilizes at a speed where the torque provided by the PWM duty cycle matches the load on the motor. Open loop control mode is typically used by sensorless BLDC systems during start up until the rotor locks into rotation and can provide sufficient BEMF for positional feedback.
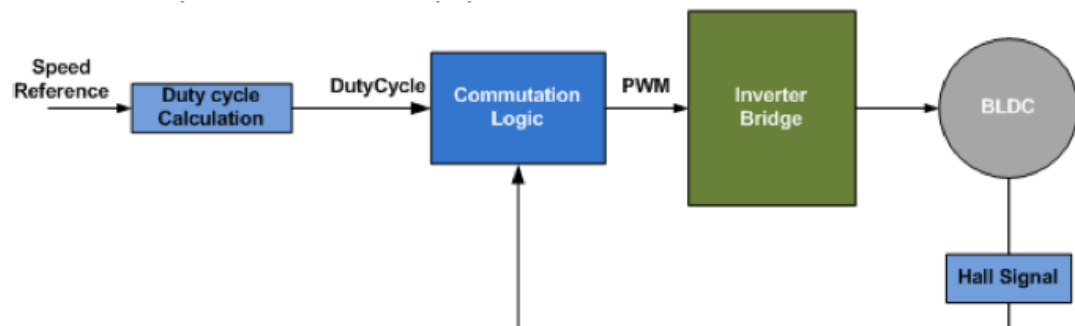

Figure 19. Open Loop Control Block Diagram [6]

29

Closed Loop Control

In closed loop control, the PWM duty cycle is calculated by a controller by measuring the actual motor velocity and comparing it with the desired velocity set by the speed reference. In the block diagram system shown in the figure below, the hall effect sensor signal is used to both drive the commutation logic and calculate the motor speed. The actual speed is compared with the speed reference, and the error value is fed into a PI controller.
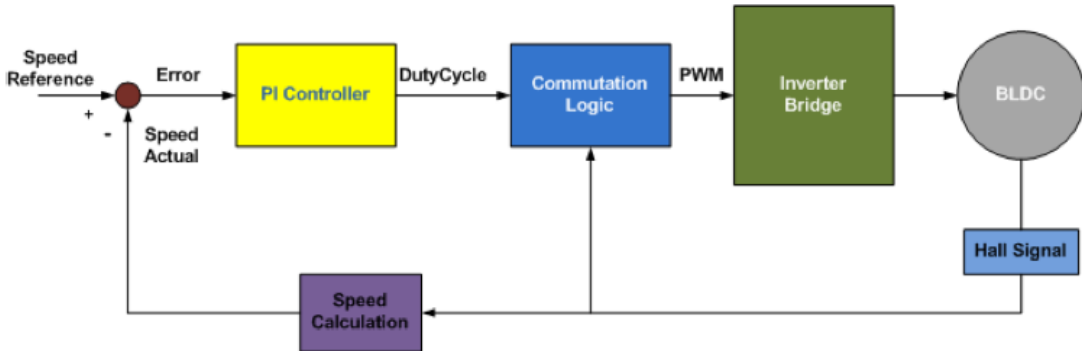
Figure 20. Closed Loop Control Block Diagram [6]

The PI controller modifies the error signal using proportional and integral gain constants to generate the PWM duty cycle.
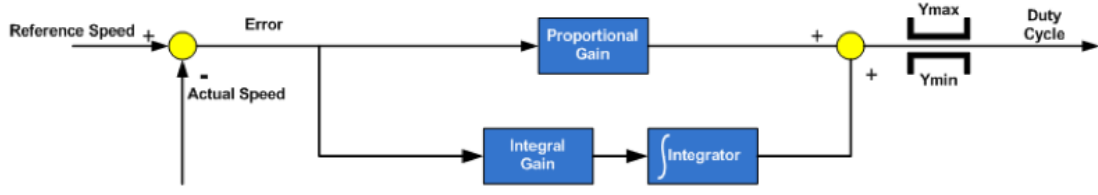
Figure 13 · Proportional-Integral Controller

Figure 21. PI Controller Block Diagram [6]

$$DutyCycle = K_p * error + K_i * \int error\, dt$$

Where K_p is the proportional gain, K_i is the integral gain, and error is the difference between the set and measured speed values.

As most calculations are done with digital microcontrollers, the following discrete time domain representation is more useful.

$$y_n(k+1) = y_n(k) + K_I * e(k)$$

$$Y_n(k+1) = y_n(k+1) + K_P * e(k)$$

Where $y_n(k+1)$ is the current integrator term, $y_n(k)$ is the previous integrator term, $e(k)$ is the different in reference speed and actual speed, and $Y_n(k+1)$ is the current computed duty cycle. [6]

### Space Vector Modulation

SVM is a popular technique used in conjunction with PWM as a control method for voltage source inverters such as those used to drive 3-phase motors. It uses space vector theory to model the 3-phase output drive and is used to control the modulation of PWM signals driving the inverter mosfet bridge between the 6 distinct commutation sectors.

Any three-phase system (with phases $a_x(t), a_y(t), a_z(t)$) can be uniquely represented as a rotating vector a_s:

$$\underline{a_S} = \frac{2}{3} \cdot \left[a_X(t) + \underline{a} \cdot a_Y(t) + \underline{a^2} \cdot a_Z(t) \right]$$

$$\text{where } \underline{a} = e^{j \cdot \frac{2\pi}{3}} \quad \text{and} \quad \underline{a^2} = e^{j \cdot \frac{4\pi}{3}}$$

The vectorial representation is obtained using the following 3/2 transformation:

$$\begin{bmatrix} A_\alpha \\ A_\beta \end{bmatrix} = \frac{2}{3} \cdot \begin{bmatrix} 1 & \frac{-1}{2} & \frac{-1}{2} \\ 0 & \frac{\sqrt{3}}{2} & -\frac{\sqrt{3}}{2} \end{bmatrix} \cdot \begin{bmatrix} a_X \\ a_Y \\ a_Z \end{bmatrix}$$

This mapping of the system in the complex plane allows for analysis of the system as a whole rather than each individual phase.

SVM Source: [5]

Vector	A^+	B^+	C^+	A^-	B^-	C^-	V_{AB}	V_{BC}	V_{CA}	
$V_0 = \{000\}$	OFF	OFF	OFF	ON	ON	ON	0	0	0	zero vector
$V_1 = \{100\}$	ON	OFF	OFF	OFF	ON	ON	$+V_{dc}$	0	$-V_{dc}$	active vector
$V_2 = \{110\}$	ON	ON	OFF	OFF	OFF	ON	0	$+V_{dc}$	$-V_{dc}$	active vector
$V_3 = \{010\}$	OFF	ON	OFF	ON	OFF	ON	$-V_{dc}$	$+V_{dc}$	0	active vector
$V_4 = \{011\}$	OFF	ON	ON	ON	OFF	OFF	$-V_{dc}$	0	$+V_{dc}$	active vector
$V_5 = \{001\}$	OFF	OFF	ON	ON	ON	OFF	0	$-V_{dc}$	$+V_{dc}$	active vector
$V_6 = \{101\}$	ON	OFF	ON	OFF	ON	OFF	$+V_{dc}$	$-V_{dc}$	0	active vector
$V_7 = \{111\}$	ON	ON	ON	OFF	OFF	OFF	0	0	0	zero vector

Table 5. Control Vectors [12]

Looking at the inverter bridge, the mosfet pairs for each phase are controlled as complementary pairs to avoid the situation when the power supply is directly shorted. Further to this, only one pair of motor connections is to be connected to the power supply at any one time during commutation. This gives rise to six active vectors corresponding to the commutation steps. There are also two zero vectors where either all high or all low side transistors are switched on. These are shown in the table above and are indicated as vectors in the complex plane in the figure below.
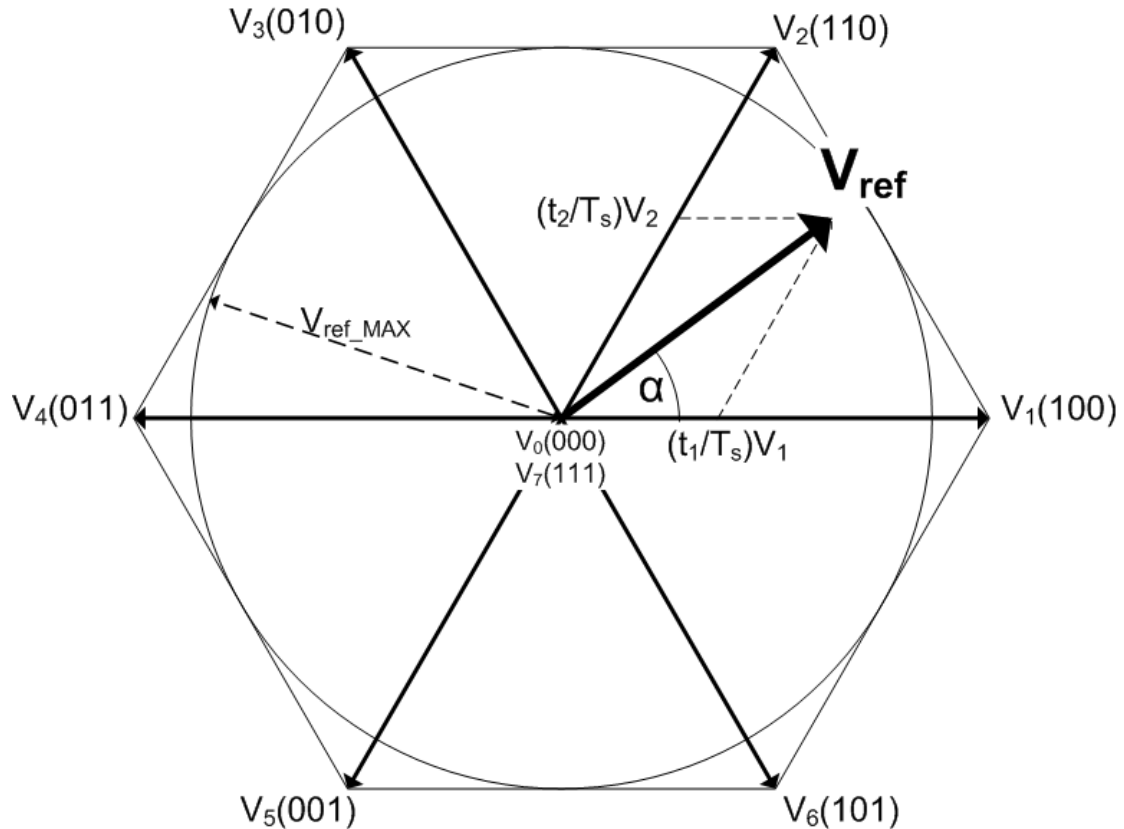
Figure 22. Space Vector Representation of a 3-phase System [12]

V_{ref} is the measured vector state of the motor as it moves within each commutation sector. With basic PWM control, only a single state vector is used to power the motor windings, with each vector covering V_{ref} positions 30° either side of their indicated positions. With Space Vector Modulation, rather than using the single vector closest to V_{ref} a combination of the two adjacent vectors and the zero vector are used instead.

$$\underline{V_S} \cdot T_S = \underline{V_a} \cdot t_a + \underline{V_b} \cdot t_b + \underline{V_0} \cdot t_0$$ where T_s is the sampling time

In the figure below, the measured V_{ref} point is at an angle of 45° closest to vector V3. It is also adjacent to vector V2 and is travelling in the counter clockwise direction. The PWM output to the inverter is a modulated combination of the zero vector, Va = V3, and Vb = V2 with $t_a \gg t_b$.

The time values are calculated using the following derived equations from [5]

$$t_a = \frac{3\,V_s}{2V_d} \cdot T_S \cdot (\cos\alpha - \frac{1}{\sqrt{3}}\sin\alpha) = \frac{\sqrt{3}\,V_s}{V_d} \cdot T_S \cdot \sin(\frac{\pi}{3} - \alpha)$$

$$t_b = \frac{\sqrt{3}\,V_s}{V_d} \cdot T_S \cdot \sin\alpha \qquad\qquad t_0 = T_S - t_a - t_b$$
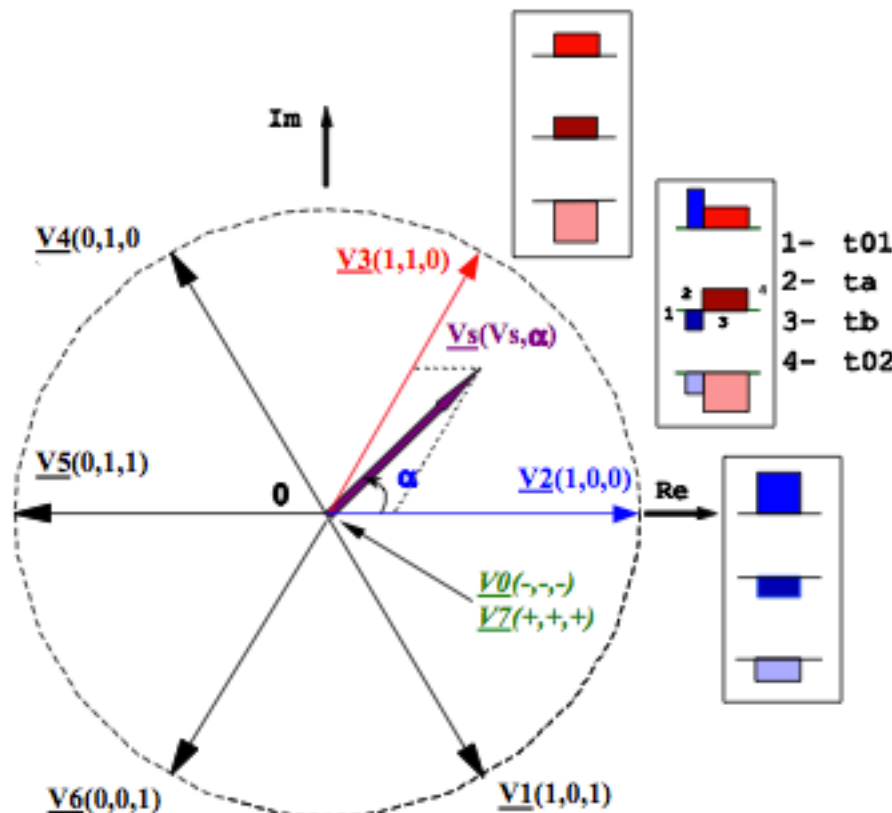

Figure 23. Space Vector Modulation Example [5]

The exact method of applying the time division across the 2 active vectors and the zero vectors can be achieved utilizing multiple methods. This includes, but is not limited to, Direct-Inverse SVM, Simple Direct SVM and Symmetrically Generated SVM. For more information on how these methods are applied see [5].

Motor and Controller Testing

Hall Effect Sensors

A testing rig has been built previously for the Turnigy motor with a hall effect sensor setup consisting of Allegro A1220 Hall Effect Latching sensors. These sensors have a minimum requirement of 40 Gauss in the worst-case scenario to trigger the latching circuit. Previous testing on the Turnigy motor has shown the strong magnets within the rotor produce a magnetic field that easily penetrates the steel can with recorded levels over 600 Gauss.
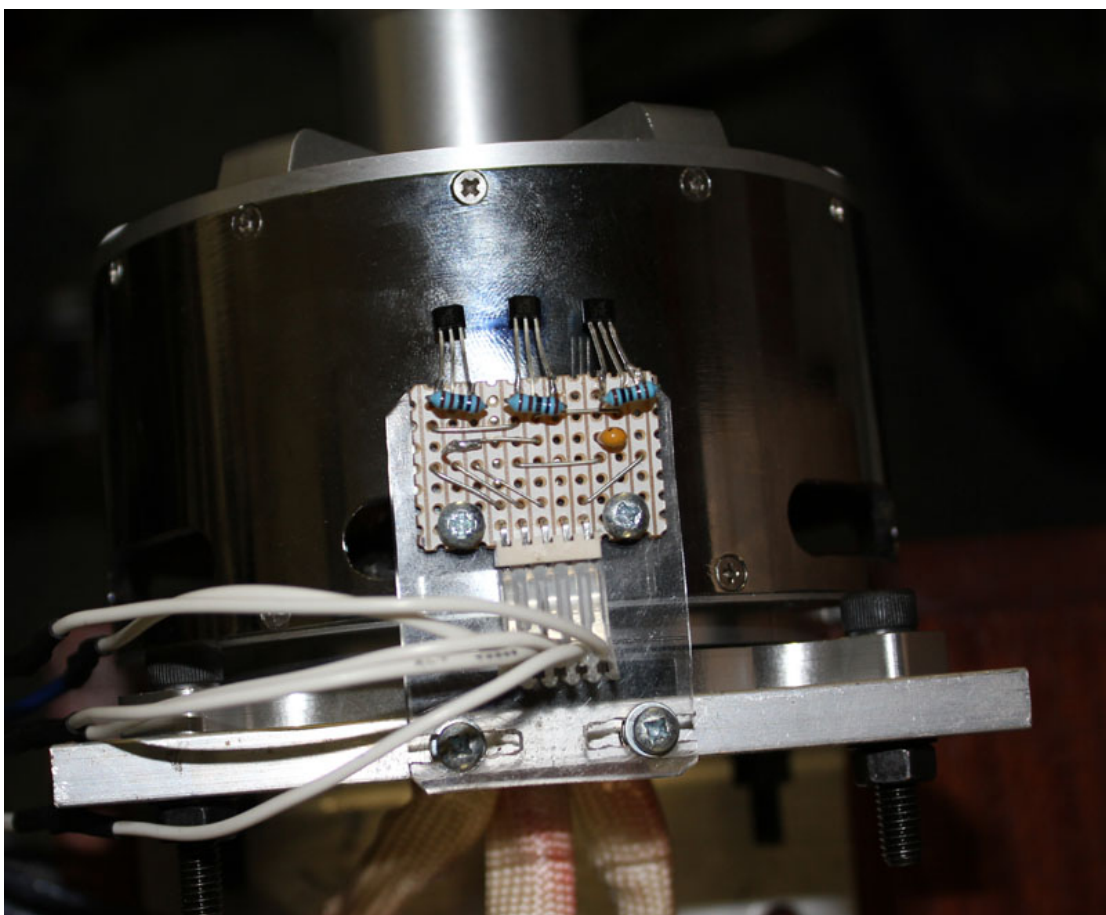

Figure 24. Hall Effect Encoder mounted on the test platform

As the Turnigy CA120-70 motor has 28 permanent magnets in the rotor, or 14 pole-pairs, there are 14 electrical cycles per complete mechanical rotation. The hall effect sensors are only used to measure each single electrical cycle to facilitate commutation. The motor physically rotates $360°/_{14} = 25.71°$ per electrical cycle so

the sensors must be evenly spaced within this section. $25.71°/_3 = 8.57°$ is the required spacing for each sensor. Sensor position can be easily verified by comparing the outputs of each hall effect sensor as the motor is turned by hand at a constant speed. The outputs of the test sensors were verified in pairs due to the use of a 2-channel oscilloscope.
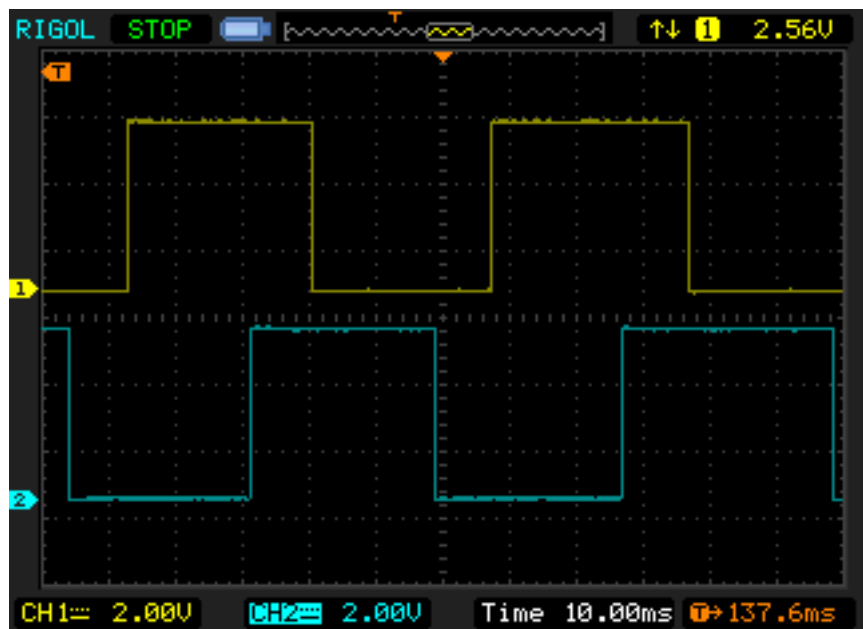

Figure 25. Hall Effect Outputs

As can be seen in the figure above, the first two sensors are 120° apart as required. A similar waveform was capture for the other two possible pairs, which were all within specification. Each output is also a 50% duty square wave as required.
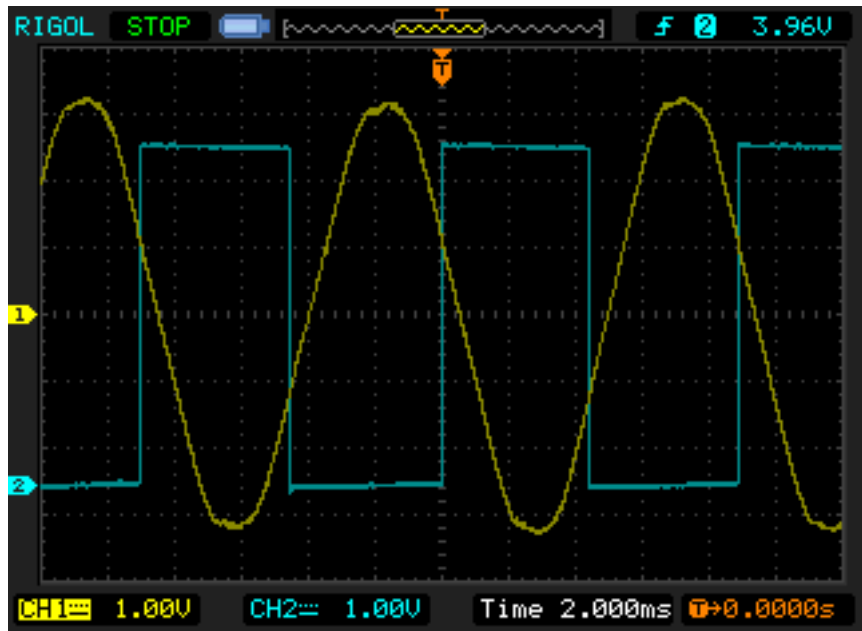
Figure 26. Hall Effect Output vs BEMF – Incorrect Alignment

Further testing was done to identify which motor connections corresponded to which hall effect output. This was achieved by rotating the motor at a fixed speed using another motorized power source, measuring the BEMF of each phase winding, and matching it with the correct hall effect output. As mentioned in the controller theory section, the hall sensor output should be a square wave representation of the BEMF.

Figure 27. Hall Effect Output vs BEMF – Correct Alignment

Motor Controllers

Initially, the decision was made to utilize SEVCON Gen4 Size 2 AC controllers. These industrial controllers are highly configu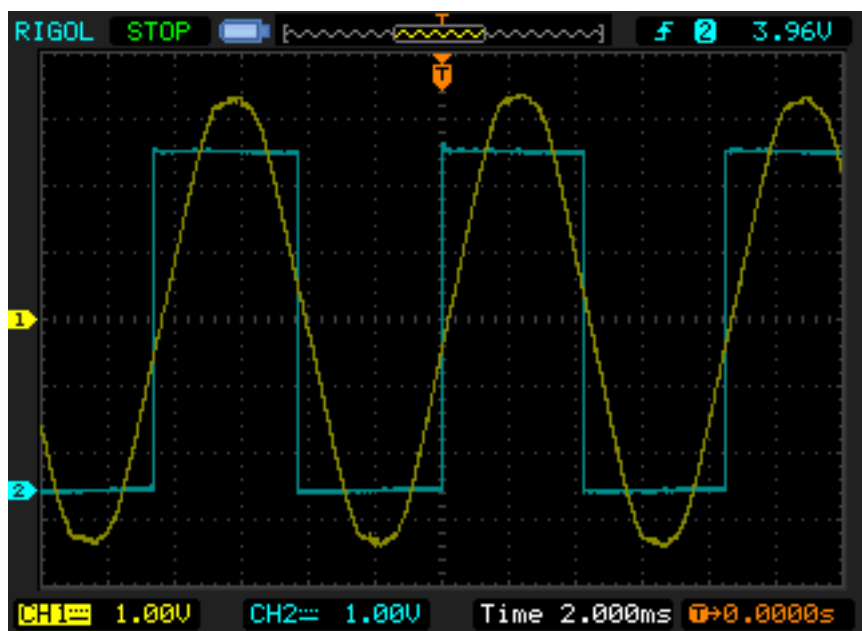rable controllers designed to drive permanent magnet AC motors or AC induction motors. They have a number of desirable features such as CAN Bus communications for interfacing with other vehicle systems, integrated contactor and various vehicle systems control, and the ability to utilize regenerative braking. However, the immense programmability of these controllers requires advanced training to configure them properly. Due to time constraints and a lack of technical knowledge about the inner workings of the controller's operational code, the decision was made to source alternative controllers. Instead of the SEVCON controllers we will be using Kelly Controls KBL72301X controllers, which are 24-72V, 300A continuous rated, BLDC controllers with regenerative braking. They have also been optioned with a CAN Bus interface to ensure compatibility with future student projects. Due to the high pole-pair count on the Turnigy motor, we needed to specify the "Ultra High Speed" option which allows for an electrical frequency up to 100,000Hz. This allows for a maximum mechanical speed of 7142 RPM based on the following equation:

$$Electrical\ RPM = Mechanical\ RPM * \#\ of\ Motor\ Pole\ Pairs$$

Figure 28. Kelly Controls BLDC Controller [14]

Small Scale Testing

While waiting for mechanical work to be completed on the vehicle and for the new motor controllers to arrive, small scale testing was performed utilizing components typically used in remote control electric aircraft.

The following components were used for testing:

Aeolian C2826 BLDC Motor

kV	1200RPM/V
Continuous Current	18A
Max Current	25A
Peak Power	235W

Turnigy MultiStar 30A Brushless ESC

This controller is based on an Atmel ATMega microcontroller, uses BEMF sensing for commutation, and uses complimentary P/N channel mosfets for the inverter bridge.
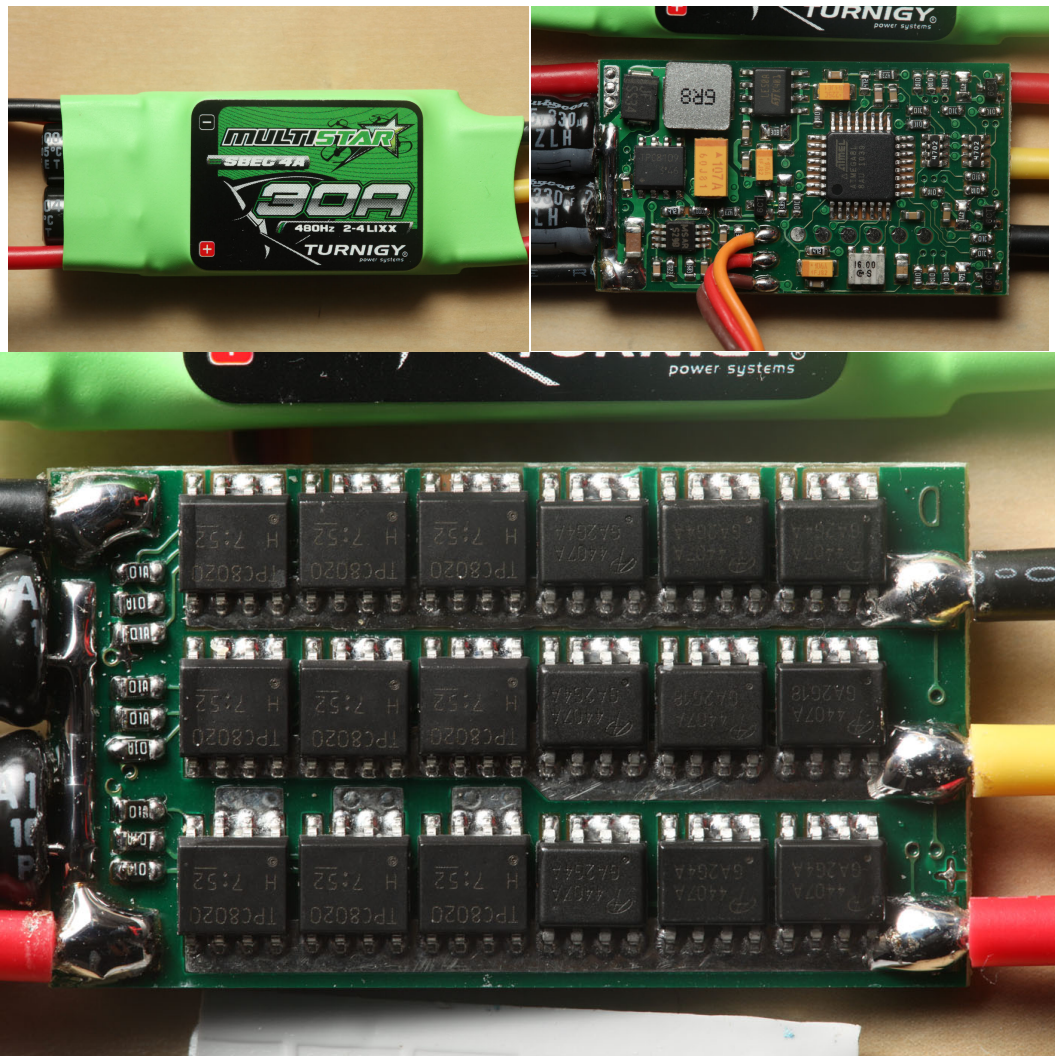
Figure 29. Turnigy MultiStar Brushless ESC

A **5030 3-blade propeller** which was used to provide the load.

Figure 30. Motor and Controller Test Setup

A Rigol DS1052e 50Mhz 2-channel Digital Oscilloscope was used to measure the outputs of the inverter bridge and the BEMF of the motor.
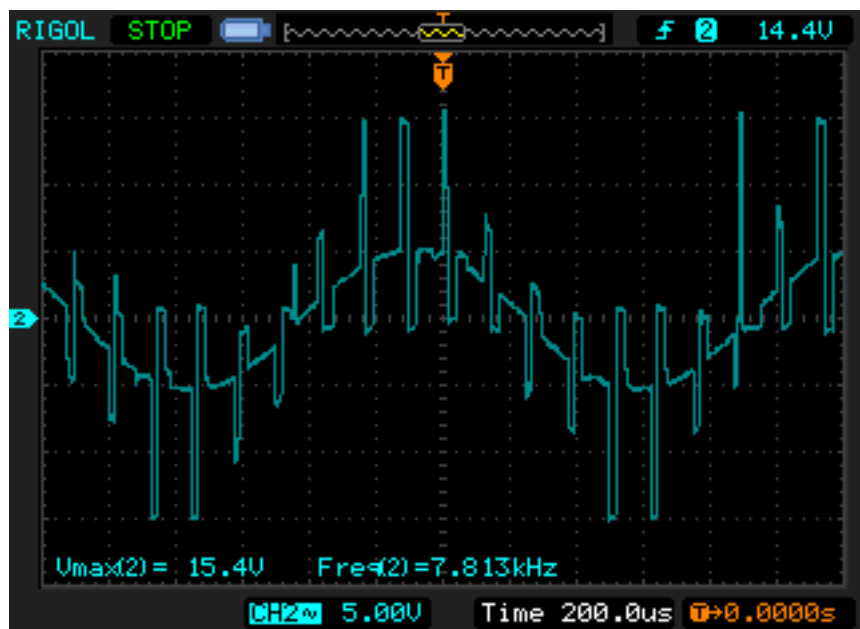
Figure 31. Phase Waveform – Low Throttle Demand

This first measurement shows the phase waveform across two terminals with a very low throttle value. The PWM switching of the inverter can be clearly seen which has

a very low duty cycle. During the T_{off} time of the PWM cycle, the BEMF waveform of the motor can be seen.

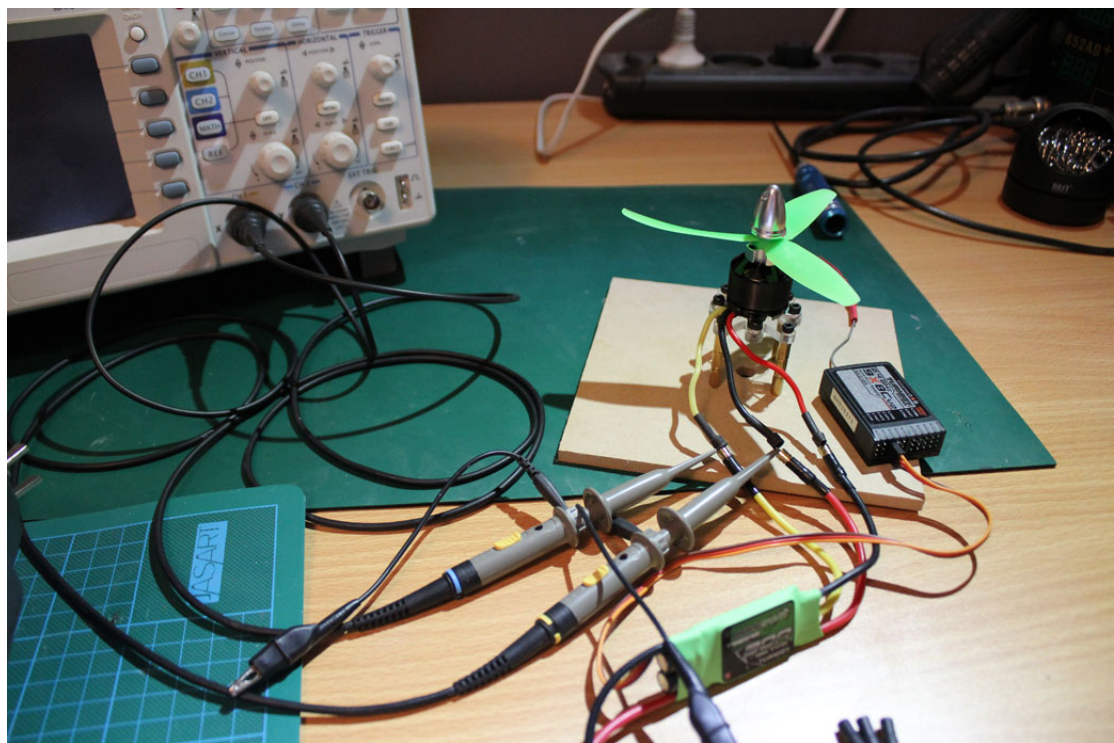*Figure 32. Phase Waveform – Medium Throttle Demand*

Increasing the throttle demand increases the PWM duty cycle and the square PWM pulses can be clearly seen with a longer T_{on} time.
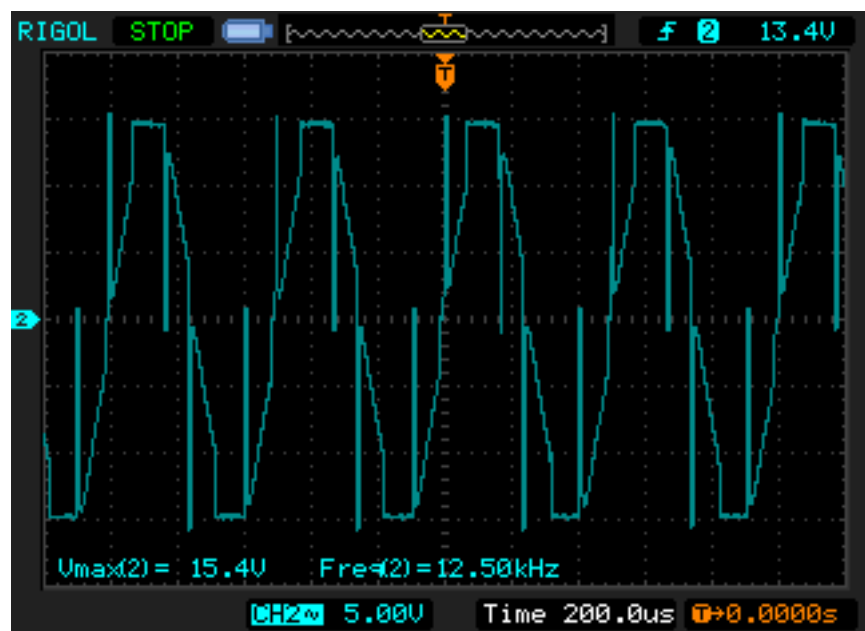
Figure 33. Phase Waveform – Full Throttle Demand

a very low duty cycle. During the T_{off} time of the PWM cycle, the BEMF waveform

42

At full throttle demand, the PWM is set to 100% duty cycle and results in the waveform above. There are distinctive peaks of positive and negative voltage each with a width of $1/6$ of each period spaced equally apart. These correspo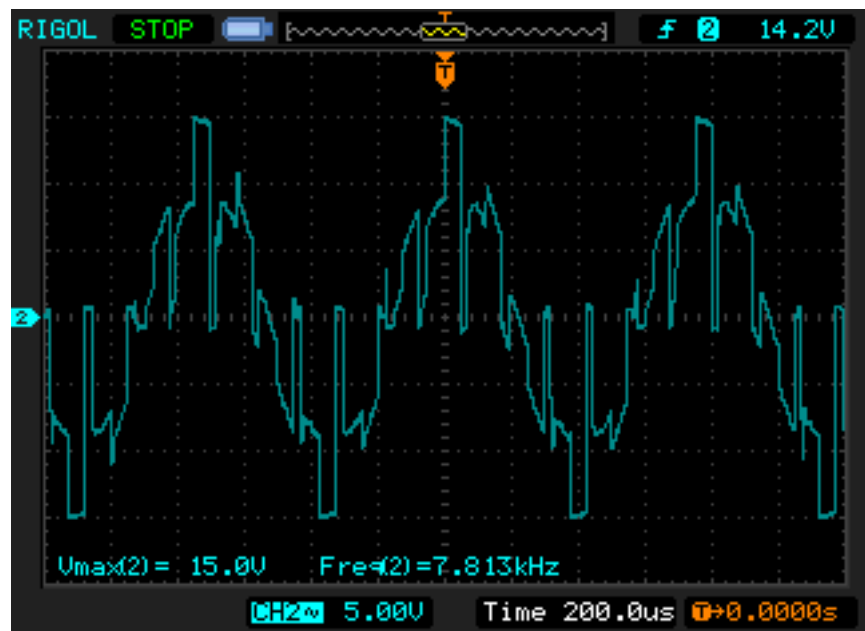nd to the two commutation sectors where current flows in each direction respectively. There is some noise due to the inductance of the motor during switch off, but the BEMF of the motor can be seen superimposed in between the voltage peaks.

Figure 34. Phase Waveform – Filtered BEMF 2 phases

Using a digital low pass filter of 5 kHZ to eliminate the commutation switching waveform, I was able to obtain the above waveform capture showing the BEMF of two phases and the 120° phase relationship between them.

43
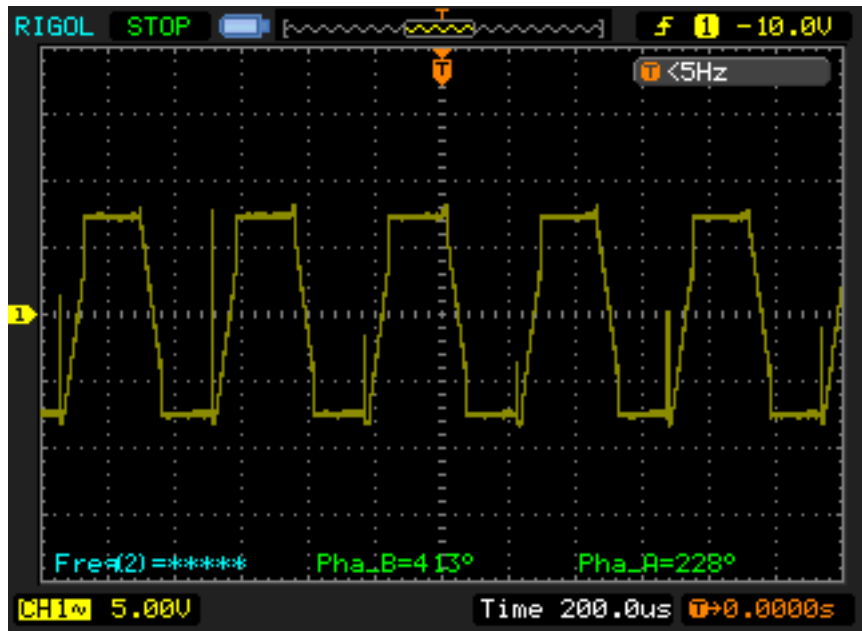
Figure 35. Inverter Output – Ground Referenced

This waveform capture shows the voltage on each inverter output relative to the negative side of the DC supply. Referring back to Table 3, each output terminal is connected to the posit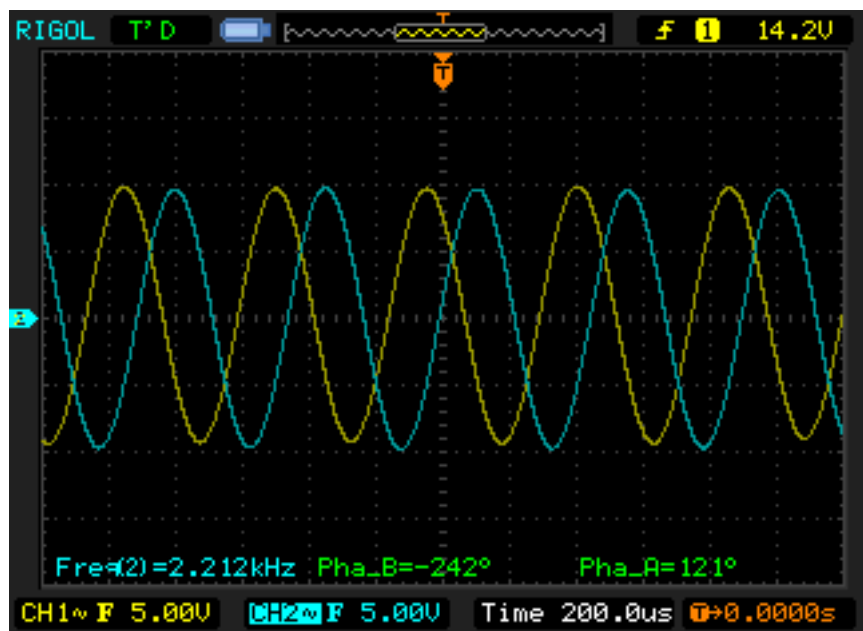ive side of the supply for two successive commutation steps. It is then left floating, before being connected to the negative side of the supply for two successive commutation steps. It is then again left floating for one step before repeating the sequence. The waveform capture above confirms what is expected from theory. There are two periods of positive voltage followed by one period where it is left floating. In the capture, this float period is shown as the slow fall time. This is actually the BEMF being captured relative to the negative DC potential. Two periods of negative voltage follow before again floating showing the BEMF.

Overall, this controller reflects the expected results based on the relevant theory. This ESC uses measurements of BEMF to identify zero crossings to synchronize the commutation steps. It does not make use of SVM instead relying on the simpler method of applying PWM to each of the six active vectors individually.

Input Signal Conditioning and Modulation

As part of the requirements of the FSAE 2012 competition, a number of rules and guidelines must be followed in order to compete. Many of these rules are related to safety and describe requirements of the system response when a failure occurs. The accelerator and brake signals form part of the safety requirement for the tractive system. An extract of the relevant section of the 2013 FSAE Draft Rules is provided in the appendix.

The accelerator, or torque encoder as it is referred to in the rules, must consist of two separate sensors that do not share supply or signal wires. If the output values of these two sensors is to deviate by more than 10%, than the system must disable power to the motors immediately until the signals are back within tolerance. Initially, we planned to use the two throttle inputs on the SEVCON controller to perform this task as the underlying control software in the controller already has the logic required to perform the validations on the input signals. However, the switch to using Kelly controllers, which only have a single throttle input, meant that a separate external circuit is required.

As the rules state that this functionality must be implemented using analog logic unless absolutely necessary, the initial idea to use a microcontroller was not feasible. Instead, the design uses a number of operational amplifiers to perform the comparison.

Another constraint is that there is only a 5V power supply rail available from the motor controllers to power this circuit, apart from the main battery which, has a nominal voltage of 48V. The circuit cannot be powered from the 12V auxiliary system unless it uses an isolated DC-DC power supply. This is because the throttle input is grounded to the high voltage negative terminal and the 12V auxiliary circuit must be isolated from it. The most viable and easiest option is to use the 5V supply. Standard op-amps usually require a dual DC supply, with a positive and a negative voltage rail. Most can however still be run on a single supply, with the negative voltage replaced by a ground connection. Initial simulations were performed using the Orcad Capture SPICE simulation tool using an LM324 opamp. The simulations revealed that the opamp should have a usable voltage output swing from 0.3V to 4.7V. Actual testing of an LM324 using a 5VDC single supply revealed the lowest

value it could output was actually only 1.9V. This was to be expected when analyzing the datasheet and consulting relevant opamp theory. This result simply proves that simulation tools are a guide and cannot be relied on without real world testing. What was required is a single supply opamp that has rail-to-rail outputs. This means the output can swing up to the rail voltage within a small margin, and down to ground potential with a minimal offset. The MicroChip MCP623x family of opamps chosen for this design can swing to within 35mV of the supply rail. This is perfect for our design as we can program the controller to have a dead zone at the upper and lower end of the range (typically 0.5V).

The actual design is split into two signal paths. As we are using single supply opamps, when subtracting the two throttle values, we may end up with a negative value. In this scenario, the output of the opamp will simply swing down to the ground rail giving a false indication that there is no difference between the two signals. Thus, we have two opamps set up as difference amplifiers with unity gain. In the first, Thottle1 is subtracted from Throttle2, and the difference output by the opamp further down the signal path. In the second, Throttle2 is subtracted from Throttle1. We now have two signals which represent the difference between the two input signals.

The second stage takes each difference signal and compares it with $^1/_{11}$ of the throttle input value. This is achieved by using a resistor divider network using a 10k resistor and a 1k resistor between the throttle signal and ground. This is 9.09% of the throttle signal. If the difference between the two throttle values is less than the 9%, then the opamp configured as a comparator will output low. If it is greater, it will output high at the full rail voltage. This satisfies the greater than 10% requirement of the rules.
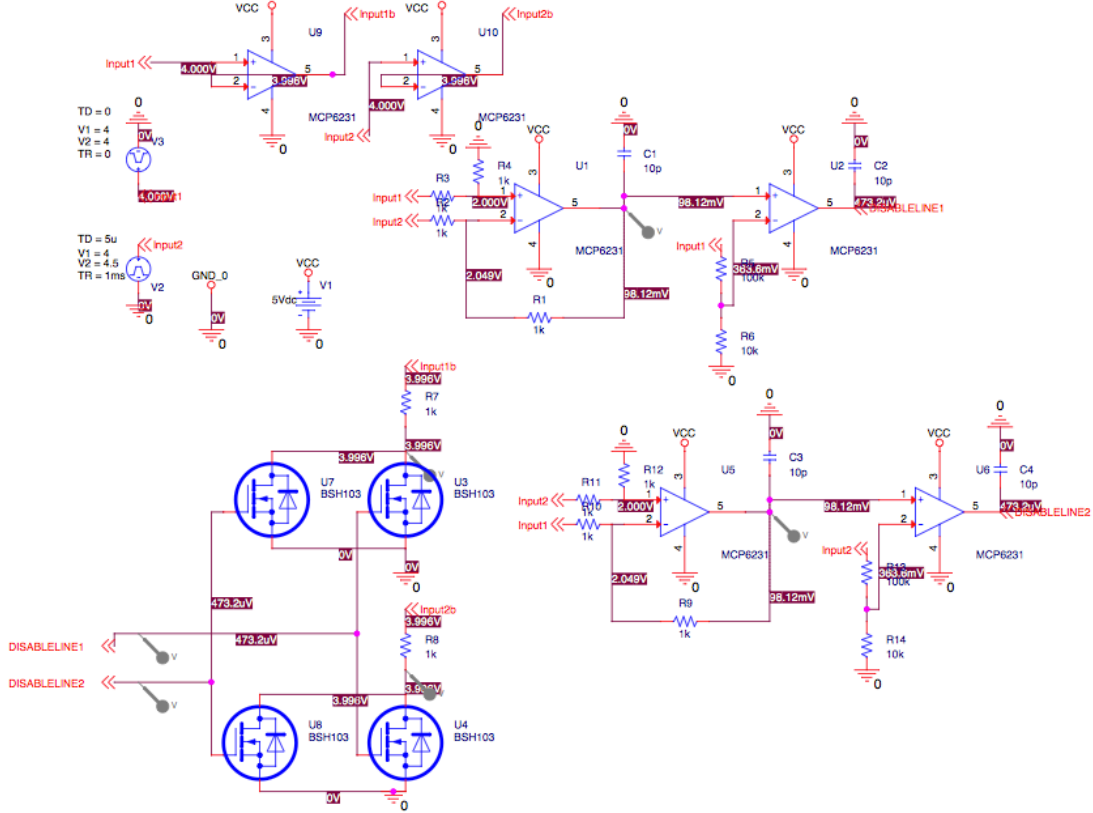
Figure 36. Input Signal Conditioning

The output of the second stage comparator is connected to a disable line which drives a pair of N channel mosfets each. The throttle signals are each buffered and output through a current limiting resistor. At this point, if the mosfets are enabled due to a disparity in the throttle signals, the buffered signal is pulled to ground and the output to the motor controllers reads as 0V.

A transient response graph of the circuit is included in the appendix. The red and green lines represent the throttle input signals, the yellow line is the disable control signal, and the pink line is the difference amplifier output. It shows the successful operation of the circuit as the output throttle signal is cut once the input signals deviate by more than 10%.

Conclusion

Due to the short time frame and the large scale of the project, a commercially available motor controller had to be chosen. A student designed controller would have been difficult due to the high voltage and currents involved. It is however important to understand the theory behind their operation in order to effectively integrate the controller into the overall system design. Accuracy and positional placement of the hall effect sensors can have a large effect on phase current and efficiency.

With strong rare earth magnets becoming widely available at cheaper prices, powerful BLDC motors are fast becoming the popular choice for applications requiring high power density with reasonable costs. The proliferation of cheap semiconductor devices and much more powerful embedded microcontrollers means advanced control algorithms can be utilized without compromising due to a lack of computational power.

Out of all the technologies being investigated for alternative energy vehicles, pure electric powered cars are highly promising. The FSAE competition and project allows students to learn about current technologies and showcase them in a competitive environment.

The current tractive system provides the foundation for a working drivable FSAE vehicle. Further testing and experimentation is required to extract its full potential.

Future Work

Motor & Controller Load Testing

The motors and controllers need to be installed into the vehicle with all the tractive wiring completed. Proper load testing must be done on the motors once all the mechanical work is complete. Previous load testing was performed on the motors using a propeller, which provides a very small load at slow speeds. When the motor is driving the FSAE vehicle it will have a must higher load from a standing start. Due to the low inductance and resistance of the motor, it will be important to ensure there is not excessive current during start up which risks damage to both controller and motor.

Hall Effect Sensor Mechanical Mount

A hall effect sensor design using surface mount Diodes Inc. AH3761 latching hall effect sensors has been proposed rather than using the through hole Allegro parts. The surface mount parts will be more resistant to shock and vibration, with the added advantage of being directly attached to the PCB for rigidity. Designs need to be finalized for the mounting position once the mechanical aspect of the wheel hubs is complete.

Drive Control Computer

Provisions have been made for the integration of a drive control computer within the vehicle system. This computer would read data from various sensors on the vehicle and use it to control the torque demand to each wheel. Some major functions would include traction control and stability control, as well as monitoring all aspect of the system. A separate replacement design for the input modulation board has been proposed that allows for external modulation of the throttle signal to each motor controller independently.

References

[1] I. Hooper, "DEVELOPMENT OF IN-WHEEL MOTOR SYSTEMS FOR FORMULA SAE ELECTRIC VEHICLES", University of Western Australia, 2011

[2] P. Yedamal, "AN885: Brushless DC (BLDC) Motor Fundamentals", MicroChip Technologies, DS00885A, 2003

[3] W. Brown, "AN857: Brushless DC Motor Control Made Easy", MicroChip Technologies, DS00857A, 2002

[4] N. Kim et al, "BLDC Motor Control Algorithm for Low-Cost Industrial Applications", IEEEXplore, 2007

[5] D. Neacsu, "Space Vector Modulation – An Introduction", Presented at IECON2001 27th Annual IEEE Conference, 2001

[6] Microsemi Corp, "Speed Control of Brushless DC Motors-Block Commutation With Hall Sensors", Microsemi Corporation, 2012

[7] Freescale Semi, "3-Phase BLDC Motor Control with Quadrature Encoder using 56F800/E", Freescale Semiconductor, 2004

[8] C. Concari & F. Troni, "Sensorless Control of BLDC Motors at Low Speed Based on Differential BEMF Measurement", IEEEXplore, 2010

[9] Image Credit. Northwestern University Mechanical. http://mechatronics.mech.northwestern.edu/design_ref/actuators/motor_theory.html

[10] Image Credit. Wikimedia Commons. http://commons.wikimedia.org/wiki/File:Wye-delta.svg

[11] Image Credit: HobbyKing. http://www.hobbyking.com

[12] Image Credit. Wikimedia Creative Commons http://en.wikipedia.org/wiki/Space_vector_modulation

[13] Distributed LRK Windings retrieved from http://www.southernsoaringclub.org.za/a-BM-motors-3.html

[14] Image Credit: Product photo available from http://kellycontroller.com/72v-brushless-kblkhb-controllers-c-23_46.html

Appendix

EV2.3.4 At least two separate sensors have to be used as torque encoder. Separate is defined as not sharing supply or signal lines.

EV2.3.5 If an implausibility occurs between the values of these two sensors the power to the motor(s) has to be immediately shut down completely. It is not necessary to completely deactivate the Tractive System, the motor controller(s) shutting down the power to the motor(s) is sufficient.

EV2.3.6 Implausibility is defined as a deviation of more than 10% pedal travel between the sensors.

EV2.3.7 If three sensors are used at least two sensors have to be within 10% pedal travel.

EV2.5 **Torque Encoder / Brake Pedal Plausibility Check**
The power to the motors has to be immediately shut down completely, if the brake pedal is actuated and the torque encoder signals more than 25% pedal travel at the same time.

EV2.5.1 The motor power shut down has to remain active until the torque encoder signals less than 5% pedal travel, no matter whether the brake pedal is still actuated or not.

Abstract from the 2013 FSAE Competition Rules Draft

Input Conditioning Circuit – Simulation Results